Structure/Function Relationships in Ligand-Based SO_2/O_2 Conversion to Sulfate As Promoted by Nickel and Palladium Thiolates

Marcetta Y. Darensbourg,* Thawatchai Tuntulani, and Joseph H. Reibenspies

Department of Chemistry, Texas A&M University, College Station, Texas 77843-3255

Received May 26, 1995[⊗]

The dithiolate complex [1,5-bis(mercaptoethyl)-1,5-diazacyclooctane]Pd(II), (bme-daco)Pd^{II} or **Pd-1**, whose structure was determined by X-ray crystallography (monoclinic $P2_1/m$ space group with $a = 6.1680(10)$ Å, $b = 15.715(5)$ Å, $c = 6.5930(10)$ Å, $\beta = 107.090(10)°$, $Z = 2$, $R = 0.0291$, $R_w = 0.0718$), has been added to a group of metal thiolates which form sulfur-site SO_2 adducts. Exposure of the **Pd-1** complex to SO_2 in methanol results in the precipitation of yellow/orange crystalline **Pd-1**·SO_2: monoclinic space group, $P2_1/c$ (No. 14), with $a = 8.928(2)$ Å, $b = 14.655(4)$ Å, $c = 11.067(2)$ Å, $\beta = 97.29(2)°$, $Z = 4$, $R = 0.0348$, $R_w = 0.0944$. Analogous thiolate–SO_2 adducts based on (bme-daco)Ni^{II}, **Ni-1**·SO_2, $(Ph_2PCH_2CH_2S)_2Ni^{II}$, **Ni-2**·$SO_2$, and (bme*-daco)$Ni^{II}$, **Ni-1***·$SO_2$, also precipitate from methanol. To explore the transformation of SO_2 to SO_4^{2-} in these adducts, the following three factors expected to control the sulfate-forming reaction have been examined: (i) the stability of SO_2 adducts; (ii) the oxidizability of the metal thiolate or its tendency to generate disulfide products on oxidation; and (iii) the ability of the metal thiolates to react with O_2 and produce sulfur-oxygenated products. The studies indicate that the last factor is the most important influence on SO_2 oxygenation. A possible mechanism involves the transient formation of an SO_2-stabilized sulfperoxide intermediate, which behaves as a nucleophile and further reacts with SO_2 to produce SO_4^{2-}. The use of the aforementioned metal thiolate complexes as catalysts for SO_2 oxygenation in the presence of a sacrificial electron donor has also been explored; simple salts such as $NiCl_2$ and $NiSO_4$ are more efficient than the complexes.

Introduction

Most recent studies of the coordination chemistry and transformations of sulfur dioxide have as a major objective the catalytic conversion of SO_2 to less noxious substances.[1] Several approaches for reducing SO_2 to sulfur and water by transition metal complexes have been developed by Kubas and co-workers.[2-8] Another process for SO_2 fixation, its oxidation to sulfate, is well-established for two-electron, oxidizable metals with abilities to form adducts of O_2 or SO_2, as in Vaska-type peroxy or SO_2 derivatives.[9,10] Both routes to metal-based SO_2 oxidation to sulfate, eqs 1 and 2, result in the formation of chelated sulfate. According to Kubas,[1] the difficult removal of chelated sulfate from the metal has impeded efforts to develop catalytic SO_2 oxidation chemistry.

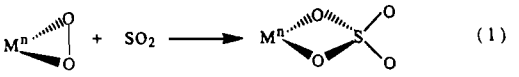

(1)

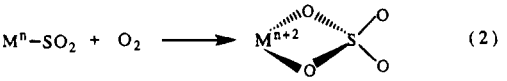

(2)

Collman and co-workers have used oxygen-18 isotopic labeling studies in search of a mechanistic understanding of SO_2 oxidation utilizing a Vaska-type iridium–oxygen complex, IrCl-$(O_2)(CO)(PPh_3)_2$, which forms coordinated sulfate, Ir(Cl)(CO)-$(SO_4)(PPh_3)_2$ (as exemplified by eq 1).[10] Proposed peroxysulfite intermediates are consistent with theoretical calculations[11] and could also be appropriate for intermediates in reaction 2. The latter metal-bound SO_2 precursor has examples in platinum(0) chemistry such as the reaction of $Pt^0(SO_2)(PPh_3)_2$ with O_2 to produce the sulfato complex $Pt^{II}(\eta^2\text{-}SO_4)(PPh_3)_2$ with concomitant two-electron oxidation of Pt^0.[9] Yet another example of the oxidation reaction of SO_2 by O_2 was reported by Poilblanc and co-workers.[12] When oxygen was bubbled into a toluene solution of $[(\mu\text{-}SCH_3)Fe(CO)_2P(CH_3)_3]_2$·$SO_2$ (an adduct presumed to contain SO_2 inserted into the Fe–Fe bond), a yellow solid characterized as SO_4-chelated $[Fe(SCH_3)(CO)_2P(CH_3)_3]_2$-$SO_4$ precipitated out of the solution. In addition, air oxidation of a bridging SO_2 in $Pt_2(\mu\text{-}SO_2)_2(C_8H_{12})_2$ was reported to form a bridging SO_3 in $Pt_2(\mu\text{-}SO_3)(\mu\text{-}SO_2)(C_8H_{12})_2$.[13]

Recently we discovered that a square planar N_2S_2 complex, (bme-daco)Ni^{II} or **Ni-1**, reacted rapidly with SO_2 to form a thiolate-sulfur-bound SO_2 adduct (bme-daco)Ni·SO_2 or **Ni-1**·SO_2, Scheme 1.[14] This structurally characterized adduct was found to react with molecular oxygen under ambient conditions to precipitate a trimetallic as its sulfate salt, $\{[(bme\text{-}daco)Ni]_2Ni\}\{SO_4\}$, from solution over the course of a few hours. Since the dithiolate complex **Ni-1** also takes up O_2 (albeit slowly) with oxygenation of thiolate sulfurs to produce very

[⊗] Abstract published in *Advance ACS Abstracts,* November 1, 1995.

(1) Kubas, G. J. *Acc. Chem. Rev.* **1994**, *27*, 183.
(2) Toupadakis, A.; Kubas, G. J.; Burns, C. J. *Inorg. Chem.* **1992**, *31*, 3810.
(3) Kubas, G. J.; Ryan, R. R.; Kubat-Martin, K. A. *J. Am. Chem. Soc.* **1989**, *111*, 7823.
(4) Kubas, G. J.; Ryan, R. R. *Polyhedron* **1986**, *5*, 473.
(5) Kubas, G. J.; Wasserman, H. J.; Ryan, R. R. *Organometallics* **1985**, *4*, 2012.
(6) Kubas, G. J.; Wasserman, H. J.; Ryan, R. *Organometallics* **1985**, *4*, 419.
(7) Kubas, G. J.; Ryan, R. R. *J. Am. Chem. Soc.* **1985**, *107*, 6138.
(8) Kubas, G. J.; Ryan, R. R. *Inorg. Chem.* **1984**, *23*, 3181.
(9) Moody, D. C.; Ryan, R. R. *Inorg. Chem.* **1977**, *16*, 1052.
(10) Valentine, J.; Valentine, D., Jr.; Collman, J. P. *Inorg. Chem.* **1971**, *10*, 219.
(11) Mehandru, S. P.; Anderson, A. B. *Inorg. Chem.* **1985**, *24*, 2570.
(12) Arabi, M. S.; Mathieu, R.; Poilblanc, R. *Inorg. Chim. Acta* **1979**, *34*, L207.
(13) Farrar, D. H.; Gukathasan, R. R. *J. Chem. Soc., Dalton Trans.* **1989**, 557.
(14) Darensbourg, M. Y.; Tuntulani, T.; Reibenspies, J. H. *Inorg. Chem.* **1994**, *33*, 611. The ligand nomenclature: bme-daco is 1,5-bis-(mercaptoethyl)-1,5-diazacyclooctane; bme*-daco is 1,5-bis(2-mercapto-2-methylpropyl)-1,5-diazacyclooctane.

0020-1669/95/1334-6287$09.00/0

Scheme 1

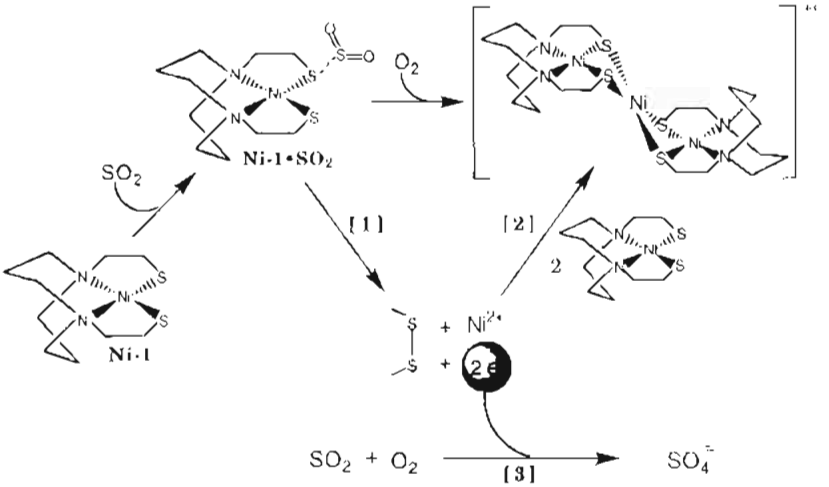

Overall Reaction: (bme-daco)Ni (s) + SO_2 (g) + O_2 (g) ⟶ {[(bme-daco)Ni]$_2$Ni}{SO_4} (s)

stable sulfinates ($NiSO_2R$),[15] the sulfate reaction could be viewed as an interception of intermediates in the S-oxygenation reaction. To our knowledge, this was the first reported example of ligand-based SO_2 oxidation by O_2 to sulfate, and Scheme 1 is given as a working hypothesis for the steps involved in this reaction.

The presence of the trimetallic species in Scheme 1 is accounted for by the oxidation of one ligand to disulfide, concomitant with the release of Ni^{2+} and two electrons (step 1). The Ni^{2+} ion is then scavenged by two parent thiolates, step 2, a step proven to be kinetically consistent with the proposed scheme. The electrons would be transferred into the combinatory process of SO_2 and O_2 to form sulfate (step 3, the "sulfate reaction"). Thus a minimum of factors which are to be prioritized in this working hypothesis, and used to expand mechanistic design, are (i) the stability of SO_2 adducts; (ii) the oxidizability of the metal thiolate or its tendency to generate disulfide products on oxidation; and (iii) the ability of metal thiolate to react with O_2 and produce sulfur-oxygenated products and their possible involvement as intermediates in SO_2 oxygenation. The following report is of attempts to establish the controlling features of this reaction. It includes examinations of other nickel thiolates such as the sterically encumbered (bme*-daco)Ni^{II}, or **Ni-1***, and $(Ph_2PCH_2CH_2S)_2Ni^{II}$, or **Ni-2**, illustrated below.[16,17] In addition, the syntheses and characterization of another group VIII metal thiolate, (bme-daco)Pd or **Pd-1**, and its ligand-bound SO_2 complex, (bme-daco)Pd·SO_2 or **Pd-1**·SO_2, are also described.

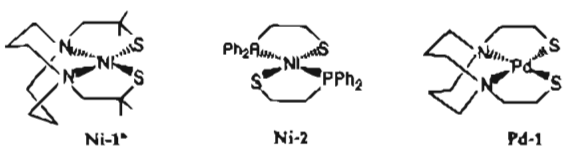

Experimental Section

Materials. Reagent-grade solvents were dried using standard techniques and distilled under N_2.[18] Palladium dichloride and CD_3OD (99.8%) were purchased from Strem Chemical Co. and Cambridge Isotope Laboratories, respectively, and used as received. Sulfur dioxide was obtained from Matheson Co. and used with no further purification. All other chemicals were purchased from Aldrich Chemical Co. and used as received. Where anaerobic conditions were required, standard Schlenk techniques using nitrogen and an argon-filled glovebox were employed.

Physical Measurements. Proton NMR spectra were recorded on a Varian XL-200 FT-NMR spectrometer. An IBM/32 FTIR spectrometer was used for the infrared spectra of SO_2 adducts taken as KBr pellets and in acetonitrile solution (0.1 mm NaCl solution cell). Vis/UV spectra were measured on a Hewlett-Packard HP8452A diode array spectrophotometer. Cyclic voltammograms were obtained using a BAS-100A electrochemical analyzer with $Ag/AgNO_3$ as reference and glassy carbon working electrodes with 0.1 M tetra-*n*-butylammonium hexafluorophosphate (TBAHFP) in CH_3CN. All cyclic voltammograms of complexes described in this paper were scaled to NHE by reference to a MeV^{2+}/MeV^{+} standard ($E_{1/2}$(NHE) = −440). Thermogravimetric analyses were carried out using a Netzsch STA-409 simultaneous thermal analyzer. Elemental analyses were carried out by Galbraith Laboratories, Inc., Knoxville, TN.

Syntheses. Ni-1, **Ni-1***, and **Ni-2** were synthesized according to published procedures.[16,17,19]

(a) (bme-daco)Pd^{II}, Pd-1. One gram of the ligand 1,5-bis(2-mercaptoethyl)-1,5-diazacyclooctane, H_2bme-daco,[19] in 25 mL of dried THF was placed in an addition funnel connected to a 50 mL Schlenk flask containing 0.22 g of NaH suspended in 10 mL of dried THF at 22 °C. The solution of H_2bme-daco was added dropwise to the suspension of NaH; the H_2 which was generated was vented via an oil bubbler. The reaction was stirred overnight, the solvent was removed in vacuo, and Na_2bme-daco was obtained as a white solid. This salt was redissolved in 25 mL of dried methanol and transferred to a suspension of 0.67 g of $PdCl_2$ in 50 mL of methanol. Black precipitates were observed after stirring for several minutes. After further stirring for 2 days, the black precipitates were removed by filtration, and the crude product was obtained upon vacuum removal of solvent. This residue was redissolved in a minimum of CH_3OH and transferred to a silica gel column, and the product was eluted with CH_3OH. The yellow solution was stripped of CH_3OH by rotary evaporation, and the resulting

(15) Farmer, P. F.; Solouki, T.; Mills, D. K.; Soma, T.; Russell, D. H.; Reibenspies, J. H.; Darensbourg, M. Y. *J. Am. Chem. Soc.* **1992**, *114*, 4601.
(16) Darensbourg, M. Y.; Font, I.; Pala, M.; Reibenspies, J. H. *J. Coord. Chem.* **1994**, *32*, 39.
(17) Hsiao, Y.-M.; Chojnacki, S. S.; Hinton, P.; Reibenspies, J. H.; Darensbourg, M. Y. *Organometallics* **1992**, *12*, 870.
(18) Gordon, A. J.; Ford, R. A. *The Chemist's Companion*; J. Wiley and Sons: New York, 1972.
(19) Mills, D. K.; Reibenspies, J. H.; Darensbourg, M. Y. *Inorg. Chem.* **1990**, *29*, 4364.

yellow solid, (bme-daco)Pd or **Pd-1**, was subsequently dried in vacuo in typical yields of 70%. ^{1}H NMR (CD_3OD) δ (ppm) for **Pd-1**: 2.15 (m, 2H), 2.43 (t, 4H), 2.60 (m, 2H), 2.77 (m, 4H), 2.92 (t, 4H), 3.13 (m, 4H). Single crystals suitable for X-ray crystal structure analysis were obtained on cooling from a hot, concentrated methanolic solution. Analytically pure samples were prepared by triturating solids of **Pd-1** with aliquots of hexane. Anal. Calcd (found): C, 35.45 (35.54); H, 5.95 (5.77); N, 8.27 (8.35). MS: (thioglycerol matrix) m/z = 339.

(b) (bme-daco)Pd·SO_2, Pd-1·SO_2. A 100 mg sample of **Pd-1** was dissolved in 20 mL of MeOH, followed by a short purge of SO_2. The yellow solid (ca. 50% yield) of **Pd-1**·SO_2, which precipitated after stirring for 5 min, was isolated in air by filtration. Single crystals suitable for X-ray crystal structure analysis were obtained by slow diffusion of ether into an SO_2-saturated DMF solution of **Pd-1**. ν(SO) (KBr) for **Pd-1**·SO_2: 1228 and 1078 cm^{-1}. Anal. Calcd (found): C, 29.81 (29.71); H, 5.00 (4.89); N, 6.95 (7.03).

Solid State Reactions of Metal Thiolate Complexes with SO_2. Powders of metal thiolate complexes (approximately 50 mg of purple **Ni-1** and **Ni-1***, yellow **Pd-1**, and green **Ni-2**) were placed into a small flask fitted with a rubber septum. The reaction flasks were flushed with SO_2. The color of the solids changed to red for **Ni-1**, **Ni-1***, and **Ni-2** and remained yellow for **Pd-1**. Weighed samples of **Ni-1**·SO_2, **Pd-1**·SO_2, **Ni-1***·SO_2, and **Ni-2**·SO_2 (ca. 50−100 mg in powdered form) were placed on an alumina crucible. Thermogravimetric analyses were carried out under N_2 atmosphere. The temperature was slowly increased (5 °C/min), and temperature vs weight change was recorded by the thermal analyzer. The percent weight loss at the first plateau was consistent to within 5% of that calculated for SO_2 loss.

Comparative Abilities of Metal Thiolate Complexes to Convert SO_2/O_2 to SO_4^{2-}. A typical reaction was carried out as follows. Approximately 100 mg of the metal thiolate was placed in a 50 mL Schlenk flask, which was subsequently degassed three times. The metal complex was dissolved in 20 mL of CH_3CN, and consequently, an excess amount of SO_2 was added by purging the solution for 20 s. Dioxygen was introduced into the reaction using an O_2-filled balloon to regulate pressure at 1 atm. The reaction was stirred under O_2 for 24 h, following which the solvent was removed in vacuo. The solid was redissolved in 10.0 mL of distilled water and transferred to a preweighed 2.5 × 20 cm test tube. A 2-fold excess of $BaCl_2$ (calculated on the basis of the metal thiolate) was added into the aqueous solution of the product to precipitate $BaSO_4$. The test tube was centrifuged for 3 min. The supernatant was discarded, the tube containing $BaSO_4$ was dried in an oven and weighed, and the yield was calculated.

Catalytic SO_2 Oxidation to SO_4^{2-}. In a 50 mL Schlenk flask, 100 mg (0.754 mmol) of NaSPh and the metal complexes (0.034 mmol) were dissolved in 20 mL of dry methanol. An excess of SO_2 was bubbled into the reaction mixture. Therewith O_2 was introduced to the reaction, employing a balloon to control O_2 pressure at 1 atm, and the reaction mixture was left to stand for 24 h. The solvent was then removed in vacuo, and the mixture was redissolved in 10.0 mL of distilled water. Undissolved NaSPh was isolated from the mixture by filtration into a 2.5 × 20 cm test tube. A 2-fold excess of $BaCl_2$ was added into the aqueous solution, and the white $BaSO_4$ which precipitated was isolated as described above. The calculated yield of $BaSO_4$ was based on NaSPh.

Reactions of [1-(2-Mercapto-2-methylpropyl)-5-(2-sulfeno-2-methylpropyl)-1,5-diazacyclooctanato]nickel(II) (Ni-1*(S_2O)) and 1,5-Bis(2-sulfeno-2-methylpropyl)-1,5-diazacyclooctanato]-nickel(II) (Ni-1*(S_2O_2)) with SO_2. A methanolic solution (15 mL) of **Ni-1***(S_2O) (30 mg) was purged with SO_2 gas. The reaction was stirred for 24 h, followed by solvent removal by rotary evaporation. The products were redissolved in CH_3OH and separated on a silica gel chromatography column eluted with CH_3OH. The products separated in the following order: the dithiolate complex **Ni-1*** (70%) and the starting **Ni-1***(S_2O) (30%). Under the same conditions, from reaction of 25 mg of **Ni-1***(S_2O_2) and SO_2 gas, the dithiolate **Ni-1*** (61%) and the monosulfoxide complex **Ni-1***(S_2O) (38%) were recovered.

The reactions of **Ni-1***(S_2O) and **Ni-1***(S_2O_2) with SO_2 described above were monitored by ^{1}H NMR. A 5 mg sample of a metallosulfoxide complex in 0.7 mL of deuterated methanol (CD_3OD) was placed in a 5 mm NMR tube, sealed with a rubber septum. Sulfur dioxide was bubbled into the NMR solution for 20 s. Subsequently, ^{1}H NMR measurements were recorded at room temperature, immediately and at 24 h intervals.

Table 1. Summary of X-ray Crystal Structure Data for **Pd-1** and **Pd-1**·SO_2

chemical formula	$C_{10}H_{20}N_2S_2Pd$, **Pd-1**	$C_{10}H_{20}N_2S_3O_2Pd$, **Pd-1**·SO_2
fw	338.80	402.88
space group	$P2_1/m$	$P2_1/c$ (No. 14)
a (Å)	6.1680(10)	8.928(2)
b (Å)	15.715(5)	14.655(4)
c (Å)	6.5930(10)	11.067(2)
β (deg)	107.090(10)	97.29(2)
V (Å^3)	610.8(2)	1436.3(6)
Z	2	4
ρ (calcd, g/cm^3)	1.842	1.715
abs coeff (mm^{-1})	1.830	13.091
goodness of fit	1.074	1.148
R^a	0.0291	0.0348
$R_w{}^a$	0.0718	0.0944

^{a} Residuals: $R = \sum|F_o - F_c|/\sum F_o$; $R_w = \{[\sum w(F_o - F_c)^2]/[\sum w(F_o)^2]\}^{1/2}$.

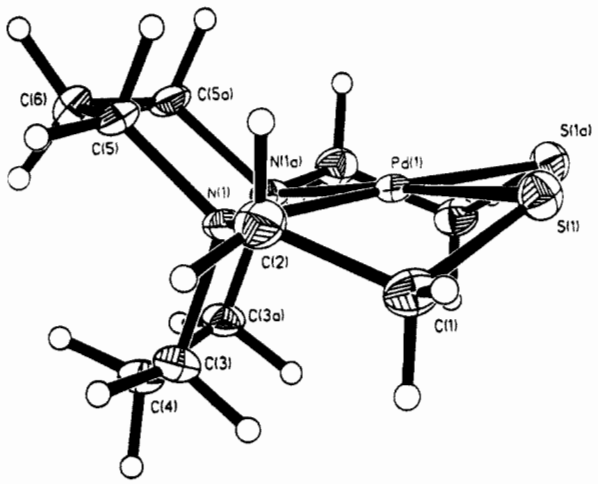

Figure 1. ORTEP plot (50% probability) representing the molecular structure of **Pd-1**. The atoms labeled a are related by a crystallographic center of symmetry. Selected bond lengths (Å): Pd(1)−S(1) 2.2795(11); Pd(1)−N(1) 2.093(3). Selected bond angles (deg): S(1)−Pd(1)−S(1a) 94.69(6); S(1)−Pd(1)−N(1) 89.05(10); S(1)−Pd(1)−N(1a) 175.19(9); N(1)−Pd(1)−N(1a) 87.1(2).

X-ray Crystal Analyses. Orange crystals of **Pd-1**·SO_2 (needle, dimensions 0.11 × 0.12 × 0.34 mm) and **Pd-1** (plate, dimensions 0.30 × 0.30 × 0.05 mm) were mounted on a glass fiber with epoxy cement at room temperature, and those of **Pd-1** were cooled to 163 K in a N_2 cold stream. Preliminary examination and data collections were performed on a Nicolet R3m/V X-ray diffractometer using Mo Kα radiation (λ = 0.710 73 Å) for **Pd-1** and a Rigaku AFC5R X-ray diffractometer using Cu Kα radiation (λ = 1.541 78 Å) in the case of **Pd-1**·SO_2. All crystallographic calculations were performed with use of the Siemens SHELXTL PLUS program package. The structures were solved by direct methods. Anisotropic refinement for all non-hydrogen atoms was done by a full-matrix least-squares method. Cell parameter and data collection summaries for both complexes are given in Table 1.

Results and Discussion

Preparation/Isolation/Characterization of Pd-1·SO_2 and Comparison to Other SO_2 Adducts of Group VIII Thiolates. The nickel thiolates used in this study have been previously reported.[16,17,19] The palladium derivative of 1,5-bis(2-mercaptoethyl)-1,5-diazacyclooctane, prepared by the reaction of $PdCl_2$ and the sodium salt of the ligand, has been characterized by X-ray crystallography to be a square planar N_2S_2 monomeric complex as shown in Figure 1. The **Pd-1** complex crystallized in a monoclinic space group, $P2_1/m$. The molecule possesses a mirror plane oriented through Pd(1), C(4), and C(6), thus

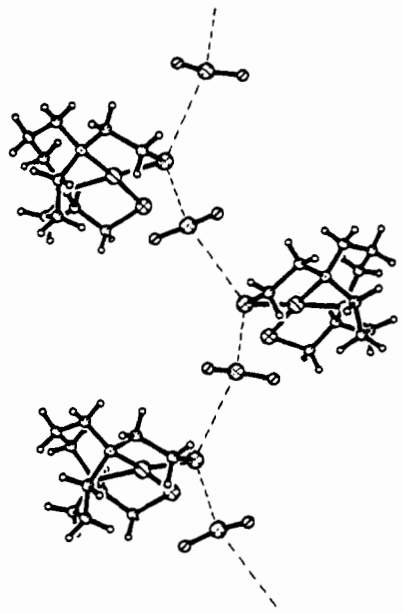

Figure 2. Portion of the packing diagram of **Pd-1**·SO_2.

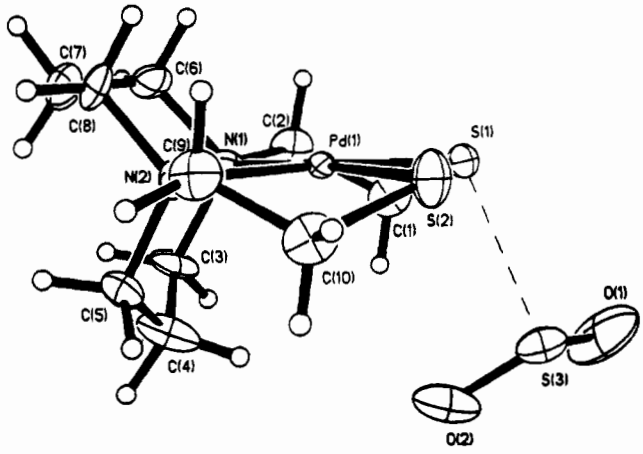

Figure 3. ORTEP plot (50% probability) representing the molecular structure of **Pd-1**·SO_2. Selected bond lengths (Å): Pd(1)−S(1) 2.2640(13); Pd(1)−S(2) 2.2671(13); Pd(1)−N(1) 2.101(4); Pd(1)−N(2) 2.087(4); S(1)−S(3) 2.588(2); S(3)−O(1) 1.423(5); S(3)−O(2) 1.439(5). Selected bond angles (deg): S(1)−Pd(1)−S(2) 94.18(5); S(1)−Pd(1)−N(1) 88.89(12); S(1)−Pd(1)−N(2) 175.03(11); S(2)−Pd(1)−N(1) 175.37(11); S(2)−Pd(1)−N(2) 89.09(12); N(1)−Pd(1)−N(2) 87.6(2); Pd(1)−S(1)−S(3) 103.2; O(1)−S(3)−O(2) 114.0(3).

generating two equivalent Pd--S and Pd--N distances, which are found to be 2.2795(11) and 2.093(3) Å, respectively. Unlike **Ni-1**, the orientation of the ethylene linkages between N and S in **Pd-1** eclipse each other across the N_2S_2 plane, and surprisingly, the diazacyclooctane framework produces two fused six-membered $PdN_2CH_2CH_2CH_2N$ rings in a chair/chair configuration. This configuration is unusual for four-coordinated metal bme-daco complexes; however, it is typical of six-coordinate derivatives of **Ni-1**.[20,21] Earlier molecular mechanics calculations of a methylated derivative of **Ni-1** found the differences in energies of the chair/chair and the chair/boat conformers to be insignificant, despite the predominance of the latter in the solid state structures.[21] The **Pd-1** complex is air stable, diamagnetic, and, unlike the deep purple **Ni-1** and **Ni-1***, a bright yellow/orange in color.

Both **Ni-1** and **Pd-1** readily take up SO_2 in solution and in the solid state. Exposures of methanolic solutions to SO_2 result in precipitation of crystalline solids, red **Ni-1**·SO_2 and yellow **Pd-1**·SO_2, which withstand removal of solvent and extended vacuum drying (ca. 0.5 Torr overnight).

Crystals of **Pd-1**·SO_2 suitable for X-ray crystallographic analysis were obtained from ether/DMF solution. Both **Pd-1**·SO_2 and **Ni-1**·SO_2 compounds crystallize in the space group $P2_1/c$ (No. 14), with almost identical crystal parameters.[14] A portion of the packing diagram for **Pd-1**·SO_2 is presented in Figure 2, and an ORTEP of a single unit, with an atom-numbering scheme, is shown in Figure 3. The PdN_2S_2 atoms are substantially planar, and the difference between the two Pd−S bond distances is not statistically significant; they average to 2.266 Å. The orientation of the ethylene linkages between N and S eclipse each other across the N_2S_2 plane, and the diazacyclooctane framework produces two fused six-membered $PdNCH_2CH_2CH_2N$ rings in the common chair/boat configuration.

As seen in Figure 2, a chain of SO_2 molecules runs through the **Pd-1**·SO_2 crystal, with one thiolate in each **Pd-1** unit bridging two SO_2 units, producing two $S_{(thiolate)}$---$S_{(SO_2)}$ contacts within the sum of S---S van der Waals radii (3.6 Å).[22] A similar situation exists for **Ni-1**·SO_2. The shorter $S_{(thiolate)}$---$S_{(SO_2)}$ bond distances are 2.588(2) Å for **Pd-1**·SO_2 and 2.597(2) Å for **Ni-1**·SO_2.[14] The second close contact of $S_{(thiolate)}$---$S_{(SO_2)}$ is 1 Å longer, with 3.592(2) Å for **Pd-1**·SO_2 and 3.692(2) Å for **Ni-1**·SO_2.

The portion of the structure and data pertinent for analysis of the geometry of SO_2 binding in **Pd-1**·SO_2 are given below.

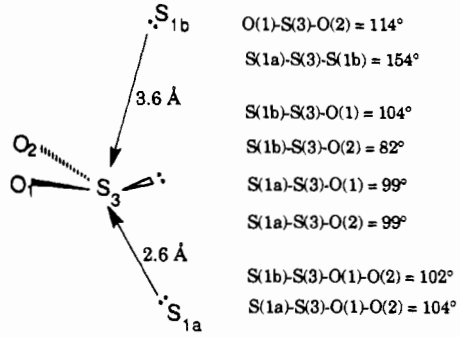

Considering only the shorter or 2.6 Å S(1)---S(2) interaction, the SO_2 unit for **Pd-1**·SO_2 appears to be in good pyramidal geometry, similar to the S-ligand-based adducts $Cu(PPh_2Me)_3$-$S(SO_2)Ph$ and $CpRu(PPh_3)(SO_2)(S(SO_2)$-4-$C_6H_4Me)$, which do not have the bridging SO_2 effect.[23,24] The average S−O bond lengths are 1.43 Å, and ∠O−S−O = 114.0°, similar to the copper and ruthenium adducts. The 3.6 Å interaction of the second thiolate sulfur does not seem to greatly influence the SO_2 unit in **Pd-1**·SO_2 toward the "sawhorse" geometry (that geometry expected for four-coordinate sulfur, as in SF_4).[25] Rather, the nucleophilicity of the second thiolate sulfur toward the SO_2 center produces a distorted tetrahedron with questionable positioning of the SO_2 sulfur lone pair.

The pattern and resonance positions of the ^1H NMR spectrum of **Pd-1**·SO_2 appear almost identical to those of **Pd-1**, indicating either little perturbation of the nearest protons by the loosely bound SO_2 group or an equilibrium with unbound SO_2. Consistently, the electronic absorption spectrum of **Pd-1** vs **Pd-1**·SO_2 shows only a minor shift in the visible region, from 343 nm (ϵ = 993) for the former to 332 nm (ϵ = 12 600) for the

(20) Goodman, D. C.; Tuntulani, T.; Reibenspies, J. H.; Farmer, P. J.; Darensbourg, M. Y. *Angew. Chem., Int. Ed. Engl.* **1992**, *32*, 116.
(21) Darensbourg, M. Y.; Font, I.; Mills, D. K.; Pala, M.; Reibenspies, J. H. *Inorg. Chem.* **1992**, *31*, 4965.
(22) Huheey, J. E. *Inorganic Chemistry: Principles of Structure and Reactivity*, 3rd ed.; Harper Collins: New York, 1983.
(23) Eller, P. G.; Kubas, G. J. *J. Am. Chem. Soc.* **1977**, *99*, 4346.
(24) Shaver, A.; Plouffe, P.-Y. *Inorg. Chem.* **1992**, *31*, 1823.
(25) Gillespie, R. J.; Hargittai, I. *The VSEPR Model of Molecular Geometry*; Allyn and Bacon: Boston, 1991; p 141.

Table 2. Thermogravimetric and Infrared Data of SO_2 Adducts

compound	SO_2 loss temp (°C) range	ν(SO) (cm^{-1})
Ni-1·SO_2	39–200	1217, 1075 (vs)
Ni-1*·SO_2	34–121	1255, 1130 (med)
Ni-2·SO_2	17–55	*a*
Pd-1·SO_2	34–162	1218, 1078 (vs)

[a] Loss of SO_2 from the complex during the KBr pellet preparation.

latter. The palladium complex shows a larger change in molar absorptivity coefficient on binding of the SO_2 than do the nickel analogues. However, the **Ni-1**, 506 nm (ϵ = 640), and **Ni-1**·SO_2, 362 nm (ϵ = 1570), pair shows a greater blue shift on formation of the adduct.

The lowering of ν(SO) frequency in the infrared spectrum (from 1340 and 1150 cm^{-1}, ν_{asym} and ν_{sym}, respectively, in free SO_2) is characteristic of binding of SO_2 through S as an electrophile.[26,27] As seen in Table 2, the solid state spectra of **Ni-1**·SO_2 and **Pd-1**·SO_2 show almost identical shifts of ca. 120 and 75 cm^{-1} in the two bands ascribed to ν_{asym} and ν_{sym}, respectively, suggesting a similar binding strength, consistent with the 2.6 Å S---SO_2 bond distance in both adducts. The ν(SO) shifts of the sterically encumbered **Ni-1***·SO_2 are only 85 and 20 cm^{-1}, for ν_{asym} and ν_{sym}, respectively, whereas **Ni-2**·SO_2 was too unstable for measurement.

Solid State Stability. The stability to vacuum of **Ni-1**·SO_2 and **Pd-1**·SO_2 is in sharp contrast to the **Ni-1***·SO_2 and **Ni-2**·SO_2 adducts, which also precipitate out of methanol but readily lose SO_2, even on attempts to remove solvent by gravity filtration. However, both **Ni-1***·SO_2 and **Ni-2**·SO_2 can be obtained as solids by reaction of powders of **Ni-1*** and **Ni-2**, respectively, with SO_2. The ν(SO) IR data for this series and the crystal-packing observations for **Ni-1**·SO_2 and **Pd-1**·SO_2 are compatible with thermogravimetric analysis data, Table 2. The onset of SO_2 loss from powders of **Ni-1**·SO_2, **Ni-1***·SO_2, and **Pd-1**·SO_2 occurs between 34 and 39 °C in all cases; however, completion of SO_2 loss varies and correlates to the IR indicator of SO_2 binding strength. The greater lability of SO_2 in **Ni-1***·SO_2 as compared to **Ni-1**·SO_2 and **Pd-1**·SO_2 can be rationalized by the steric effect of the tetramethylated analogue of **Ni-1**, since the electronic effect of the electron-donating substituents should be to enhance the S---SO_2 interaction.

Despite almost identical infrared ν(SO) values and the crystal packings for **Ni-1**·SO_2 and **Pd-1**·SO_2, the completion of SO_2 loss of **Ni-1**·SO_2 occurs at ca. 40 °C higher than that of **Pd-1**·SO_2. On the basis of other indicators of S-nucleophilicity in the parent dithiolates, such as rates of methylation and the accessibility of S-electrons by electrochemical measurements, we suggest that this difference in thermal stability reflects an electronic effect. The relief of the group VIII metal d_π–sulfur lone pair π^* interaction[28] is greater for the smaller nickel.

d_π-sulfur lone pair π^* interaction

The phosphino/thiolate **Ni-2** complex shows the lowest temperature for SO_2 loss of the four complexes. Since both the donor set and the stereochemistry of this complex differ from the other three, speculations as to its poor ability to bind SO_2 are unwarranted. It should be noted that an extensive series of *trans*-R_3PCuSR'/SO_2 adducts showed that better donors, both R at phosphorus and R′ at sulfur, enhanced R′S---SO_2 interaction.[23]

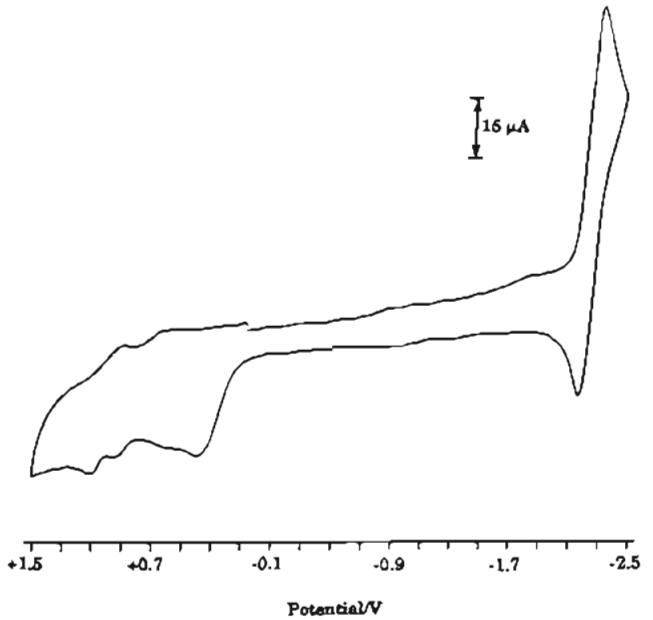

Figure 4. Cyclic voltammograph of **Pd-1** using 0.1 M TBAHFP as an electrolyte in CH_3CN.

Solution State Stability. The solution stability of the nickel thiolate·SO_2 adducts was compared in acetonitrile (the **Pd-1**·SO_2 precipitates from the concentrated solution) by the persistence of SO_2 adducts while Ar or N_2 was bubbled through the solution. Under approximately identical conditions, the time required to remove SO_2 ranged from 10 to 60 min, yielding a solution stability order as follows:

$$\text{Ni}-1\cdot SO_2 > \text{Ni}-1^*SO_2 > \text{Ni}-2\cdot SO_2$$

Electrochemical Studies. Cyclic voltammographs (CVs) of **Ni-1**, **Ni-1***, and **Ni-2** have been previously reported.[17,29,30] All except **Ni-2** show reversible reduction potentials assigned to the $Ni^{II/I}$ couple. An irreversible anodic event ascribed to the oxidation of thiolate sulfur to disulfide was found in all complexes. This presumption is supported by the fact that in one case of oxidation of nickel thiolates by 2 equiv of a one-electron oxidant the disulfide was isolated and identified.[14] The CV of **Pd-1** is shown in Figure 4. A quasi-reversible wave with $i_{p_c}/i_{p_a} = 2$ is seen at $E_{1/2} = -2188$ (ΔE = 74 mV) and is assigned to $Pd^{II/I}$. An irreversible oxidation is seen at +389 mV, referenced to NHE using methylviologen as a standard. Thus, the accessibility of the oxidation potential of the complexes (or the ease of oxidizing the ligand to disulfide) decreases as follows:

	Ni-1*	>	**Ni-1**	>	**Pd-1**	>	**Ni-2**
$E_{pa(irr.\ ox.)}$ (mV)	280		360		390		396
$E_{1/2(rev.\ M^{II/I})}$ (mV)	−2140		−1944		−2188		

(26) Byler, D. M.; Shriver, D. F. *Inorg. Chem.* **1976**, *15*, 32.
(27) Kubas, G. J. *Inorg. Chem.* **1979**, *18*, 182.
(28) Ashby, M. T.; Enemark, J. H.; Lichtenberger, D. L. *Inorg. Chem.* **1988**, *27*, 191.
(29) Farmer, P. J.; Reibenspies, J. H.; Lindahl, P. A.; Darensbourg, M. Y. *J. Am. Chem. Soc.* **1993**, *115*, 4665.
(30) Buonomo, R. M.; Font, I.; Maguire, M. J.; Reibenspies, J. H.; Tuntulani, T.; Darensbourg, M. Y. *J. Am. Chem. Soc.* **1995**, *117*, 963. The head gas over the reaction of **Ni-1***(S_2O) and **Ni-1***(S_2O_2) with SO_2 in CH_3CN was found by GC to have an SO_3/SO_2 ratio of 1:2, whereas a control (equivalent amount of SO_2 dissolved in CH_3CN) found the ratio to be 1:58.

Scheme 2

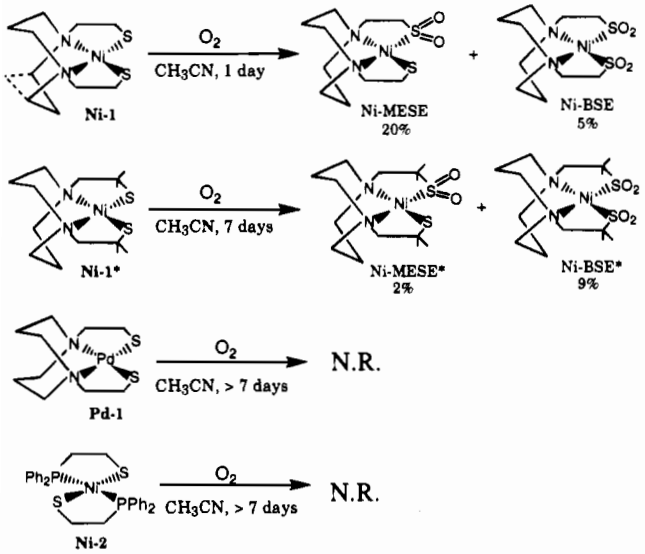

The ease of oxidation of **Ni-1***, 72 mV more accessible than the less sterically hindered analogue, **Ni-1**, is rationalized by the increased electron density at sulfur occasioned by the methyl substituents α to sulfur. On the other hand, **Ni-2** and **Pd-1**, expected to have lower electron density at thiolate sulfur, as described previously, are oxidized with greater difficulty.

Attempts to record the cyclic voltammograph of the **Ni-1**·SO_2 adduct, shown to be the most stable in the solution, were unsuccessful; the instability of the adduct in the electrolyte solution resulted in the CV characteristic of **Ni-1**.

Reaction with O_2. Under ambient conditions, **Ni-1** and **Ni-1*** react with O_2 in acetonitrile to produce monosulfone (MESE) and bis(sulfone) (BSE) complexes,[15,30] Scheme 2. In acetonitrile/water mixtures, **Ni-1** and O_2 were found to also produce a metallosulfoxide complex, Ni−S(=O)R.[31] As indicated in Scheme 2, the sterically hindered complex **Ni-1*** reacts very slowly with O_2, resulting in ca. 10% conversion over a week of reaction, whereas a 25% conversion is realized by **Ni-1** within 1 day. In contrast, **Pd-1** showed no reaction with O_2 under ambient conditions over the course of 1 week. (There is, however, reaction of **Pd-1** with O_2 in methanol when UV photolysis is employed, and the major product under these conditions is a metallosulfoxide complex.[32]) The P_2S_2 complex, **Ni-2**, does not react with O_2 either under ambient conditions or with photolysis. Therefore, the ability of metal complexes to react with O_2 and form sulfur-oxygenates as products can be ranked as follows:

$$\textbf{Ni−1} > \textbf{Ni−1*} > \textbf{Pd−1} > \textbf{Ni−2}$$

Summarization/Correlation of Factors for Sulfate Formation Reaction. As described in the Experimental Section, reactions of SO_2, O_2, and the metal thiolates, in dry CH_3CN solution, were carried out over a 24 h period. Within a few hours, dark precipitates began to form in the cases of **Ni-1** and **Ni-1***.[14] The former was identified as a sulfate salt of the trimetallic, $(\textbf{Ni-1})_2Ni^{2+}$, by UV/vis comparison with the well-characterized bromide salt.[15] FAB mass spectrometry of the nickel-containing product of the latter was found to contain a signal at $m/z = 752$, corresponding to the molecular mass of the corresponding $(\textbf{Ni-1*})_2Ni^{2+}$ ion. The IR spectra of both complexes show strong bands at 1042 and 623 cm^{-1}, characteristic of sulfate ion.[33]

Table 3. Production of Sulfate from SO_2/O_2 and Group VIII Metal Thiolates[a]

complex	amount of complex mg (mmol)	$BaSO_4$ obtained mg (mmol)	$BaSO_4$ obtained %[d]
Ni-1[b]	100 (0.343)	23.4 (0.100)	87
Ni-1*[b]	100 (0.288)	16.1 (0.069)	72
Pd-1[c]	100 (0.295)	13.0 (0.056)	57
Ni-2[b]	100 (0.182)	0	0

[a] All reactions were at 1 atm O_2, 22 °C, 24 h, and room temperature. [b] CH_3CN solvent. [c] 50% mixture of CH_3OH and CH_3CN. [d] % $BaSO_4$ obtained was based on the amount of metal complex used in the reaction.

A quantitative analysis of the sulfate production was determined by dissolution of the residue in water and precipitation as $BaSO_4$. The weighed quantities and percent yields, an average of two experiments, are given in Table 3. Sulfate production follows the order

$$\textbf{Ni−1} > \textbf{Ni−1*} > \textbf{Pd−1} > \textbf{Ni−2}$$

The results for each of the factors which are expected to control the sulfate formation reaction described thus far can be summarized as follows and compared with the reaction efficacy given by Table 3.

(1) binding of SO_2 and thermal stability to SO_2 loss

$$\textbf{Ni−1} \sim \textbf{Pd−1} > \textbf{Ni−1*} \gg \textbf{Ni−2}$$

(2) oxidizability (oxidation potential/disulfide formation)

$$\textbf{Ni−1*} > \textbf{Ni−1} > \textbf{Pd−1} > \textbf{Ni−2}$$

(3) oxidizability (O_2-reactivity)

$$\textbf{Ni−1} > \textbf{Ni−1*} > \textbf{Pd−1} > \textbf{Ni−2}$$

Clearly **Ni-2**, the poorest complex in sulfate production, is in the hindmost position for each possible determining factor. The **Pd-1** complex is in second poorest position in sulfate production, but shows an ability to bind SO_2 equal to that of **Ni-1** in the solid state. Thus we conclude that factor 1 does not substantially control sulfate production. The one-electron oxidation places **Pd-1** and **Ni-2** in synchrony with the sulfate reaction results but would place **Ni-1*** above **Ni-1**. The rank order of the complexes with regards to the individual factors which might determine relative reactivity in the sulfate production finds its best match in the O_2-reactivity scale.

Mechanistic Studies of the Sulfate Formation Reaction

As a working hypothesis, consistent with conclusions for the metal-based SO_2/O_2/sulfate reaction,[10,34] we propose that the first step in the thiolate-based sulfate reaction involves oxygen addition to the metal complexes. Whether the initial O_2-binding is at nickel (structure **A**, examples of which are found in the work of Martell et al.[35] and Kimura et al.[36]), followed by transfer to sulfur, or whether initial O_2 binding is at thiolate-

(31) Farmer, P. J.; Verpeaux, J.-N.; Amatore, C.; Darensbourg, M. Y.; Musie, G. *J. Am. Chem. Soc.* **1994**, *116*, 9355.
(32) Tuntulani, T.; Musie, G.; Darensbourg, M. Y.; Reibenspies, J. H. *Inorg. Chem.* **1995**, *34*, 6279.
(33) Nakamoto, K. *Infrared and Raman Spectra of Inorganic and Coordination Compounds*; John Wiley & Sons: New York, 1986; Vol. 4, p 484.
(34) Horn, R. W.; Weissberger, E.; Collman, J. P. *Inorg. Chem.* **1970**, 9, 2367.
(35) Chen, D.; Motekaitis, R. J.; Martell, A. E. *Inorg. Chem.* **1991**, *30*, 1396.
(36) Kimura, E.; Sakonaka, A.; Machida, R. *J. Am. Chem. Soc.* **1982**, *104*, 4255.

sulfur, is not known. Ultimately, in the absence of SO_2, S-bound oxygenates,[15,30] with expected precursor intermediates such as those illustrated by the sulfperoxide **B**, the thiadioxirane **C**,[37,38] or the dithiadioxirane **D**, are produced and isolated.

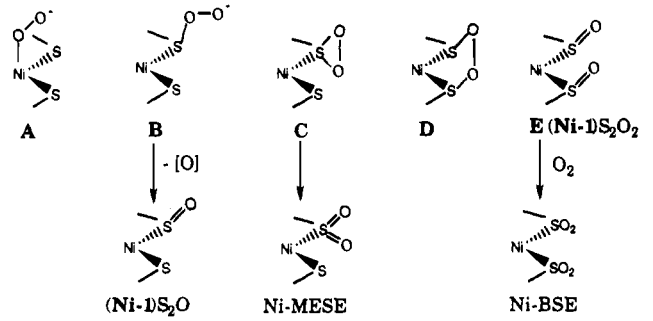

The isolated oxygenates, Ni−MESE, the bis(sulfone) complex Ni−BSE, and the metallosulfoxides (**Ni-1**)S_2O and (**Ni-1**)S_2O_2 were checked for reactivity with SO_2. In particular, the possibility of an intermediate such as structure **F**, using the bis-

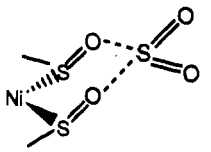

F

(sulfoxide) species **E** as a S-based analogue of the metal-based sulfate reaction described by eq 1,[10] was of interest.

Reaction of S-Oxygenated Complexes with SO_2. Metallosulfone complexes such as Ni-MESE or Ni-BSE shown in Scheme 2 do not react at all with SO_2. However, the metallosulfoxide complexes, [1-(2-mercapto-2-methylpropyl)-5-(2-sulfeno-2-methylpropyl)-1,5-diazacyclooctanato]-nickel(II), **Ni-1***(S_2O),[39] isolated from stoichiometric controlled reactions of hydrogen peroxide with **Ni-1***, or [1-(2-mercapto-ethyl)-5-(2-sulfenatoethyl)-1,5-diazacyclooctanato]nickel(II), **Ni-1**(S_2O),[31] prepared by the reaction of O_2 with **Ni-1** in aqueous media, both serve as O atom sources to SO_2, producing the parent nickel thiolates and the SO_3 molecule, which can be detected by GC/MS.[30] The reaction of **Ni-1***(S_2O) with SO_2 could be easily monitored by ^{1}H NMR and requires more than 24 h for completion. The four methyl groups in the starting material, **Ni-1***(S_2O), are all nonequivalent and thus show four resonances (Figure 5a) at 1.58, 1.48, 1.24, and 1.14 ppm, whereas the product, **Ni-1***, has four equivalent methyl groups and shows only one resonance at 1.42 ppm in the spectrum (Figure 5c). The ^{1}H NMR revealed an intermediate during the SO_3 formation ascribed to an adduct of the SO_2 bound through a sulfenate-oxygen; this intermediate displays three resonances at 1.65, 1.54, and 1.33 ppm, as shown in Figure 5b.

In the same manner, the bis(sulfoxide) complex [1,5-bis(2-sulfeno-2-methylpropyl)-1,5-diazacyclooctanato]nickel(II), **Ni-1***(S_2O_2),[30] reacts with SO_2 over the course of 1 day to give **Ni-1*** as a product (61%) and some **Ni-1***(S_2O) (38%). ^{1}H NMR reaction monitor shows that the starting material, **Ni-1***(S_2O_2), displays two resonances (Figure 6a) at 1.42 and 1.39 ppm for the two nonequivalent methyl groups; whereas the

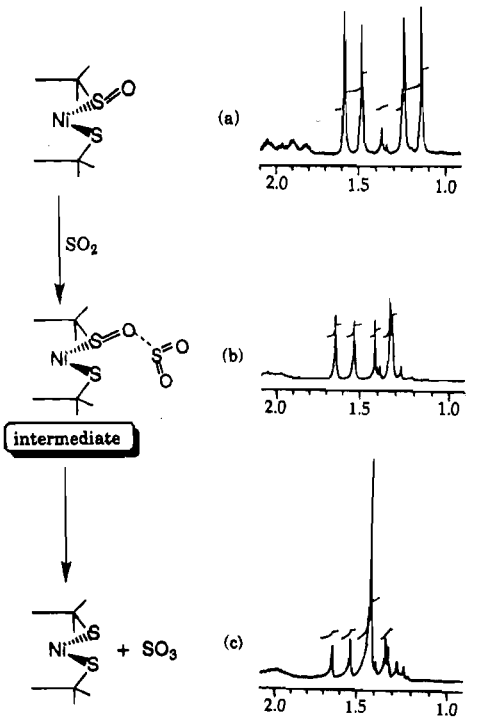

Figure 5. ^{1}H NMR monitor of the reaction of **Ni-1***(S_2O) with SO_2 in CD_3OD: (a) before addition of SO_2; (b) immediately after addition; (c) 24 h after addition.

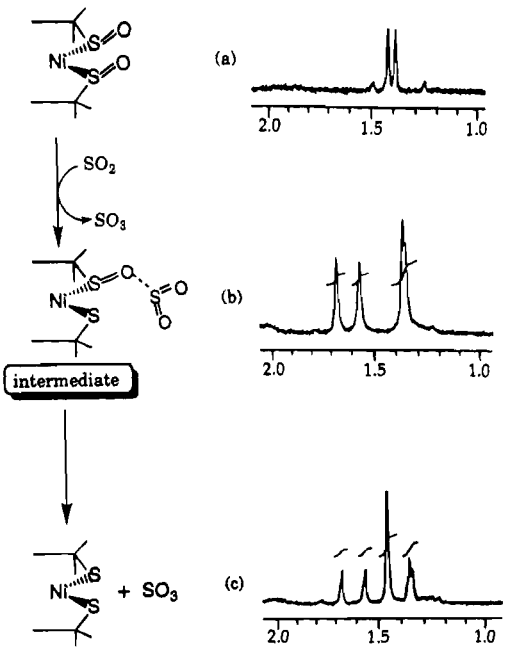

Figure 6. ^{1}H NMR monitor of the reaction of **Ni-1***(S_2O_2) with SO_2 in CD_3OD: (a) before addition of SO_2; (b) immediately after addition; (c) 24 h after addition.

product, **Ni-1***, shows only one resonance at 1.42 ppm in the spectrum (Figure 6c). The ^{1}H NMR spectrum in Figure 6b reveals an intermediate similar to that observed from the reaction of **Ni-1***(S_2O) with SO_2, *vide supra*. Thus, it can be concluded that SO_2 strips off the first O atom of **Ni-1***(S_2O_2) very rapidly to give **Ni-1***(S_2O), which then further reacts slowly with another molecule of SO_2 to produce **Ni-1*** and unreacted **Ni-1***(S_2O). Such stepwise removal of oxygen atoms by SO_2 from **Ni-1***(S_2O_2) eliminates the possibility of **D** or **E** as an intermediate in the sulfate-forming reaction, resulting in the concerted-type transition state or intermediate expressed by structure **F** above.

(37) Mirza, S. A.; Pressler, M. A.; Kumar, M.; Day, R. O.; Maroney, M. J. *Inorg. Chem.* **1993**, *32*, 977.
(38) Darensbourg, M. Y.; Farmer, P. J.; Soma, T.; Russell, D. H.; Solouki, T.; Reibenspies, J. H. In *The Activation of Dioxygen and Homogeneous Catalytic Oxidation*; Barton, D. H. R., Martell, A. E., Sawyer, D. T., Eds.; Plenum Press: New York, 1993; p 209.
(39) Font, I.; Buonomo, R.; Reibenspies, J. H.; Darensbourg, M. Y. *Inorg. Chem.* **1993**, *32*, 5897.

Scheme 3

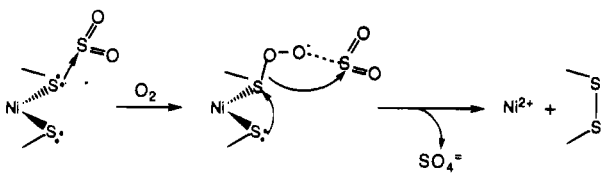

Table 4. Catalysis of $SO_2/O_2/SO_4^{2-}$ Using NaSPh as Electron Source[a]

metal	% $BaSO_4$ obtained[c]	% yield[d]
Ni-1	19.1	210
Ni-1* [b]	22.5	250
Ni-2 [b]	17.4	190
Pd-1	11.9	130
$NiCl_2$	86.4	420
$NiSO_4$	90.5	440

[a] The reactions were performed at room temperature, 1 atm O_2, for 24 h using 3.44×10^{-5} mol of the metal complex, 7.79×10^{-5} mol of the metal salt, and 7.54×10^{-4} mol of NaSPh (approximately 1:20 metal/NaSPh ratio). [b] Recovered at end of reaction period. [c] Value is based on amount of NaSPh used and is the average of two experiments. [d] Value is based on amount of metal used.

Proposed Mechanism. Although it is clear that SO_2 can remove oxygen from metallosulfoxides, the slow rates of such reactions lead us to suggest that the SO_2/O_2 interaction occurs at an earlier juncture in O_2 addition to metal-bound sulfur. All previous chemistry with **Ni-1** or **Ni-1*** shows nucleophilic reactivity at thiolate-sulfur, including alkylation,[19-21] metalation,[40,41] and as presented in this paper, the formation of S-bound SO_2 adducts. Current mechanistic studies of S-oxygenation with molecular O_2 invoke the binding of O_2 to sulfur as a sulfperoxide adduct[37,38] and find intermolecular O—O scission processes to be promoted in the presence of protic solvents. We suggest that SO_2, acting as a Lewis acid, also promotes the formation of the sulfperoxide adduct, and we will use that proposed species as a starting point for the simple mechanism outlined in Scheme 3.

The mechanism expressed in Scheme 3 is related to that proposed for formation of metal-chelated sulfate in Vaska-type complexes described by Valentine et al.[10] It involves either O_2 displacement of SO_2 or insertion of O_2 into the S(thiolate)---S(SO_2) bond, forming an SO_2-stabilized sulfperoxide species. Electron transfer concomitant with oxygen transfer generates sulfate anion and a disulfide compound. As mentioned earlier, in the case of **Ni-1*** reactions, an organic compound was isolated and characterized by ^1H NMR and mass spectrometry to be an intramolecular disulfide derivative of bme*-daco ligand.[14] This observation supports the mechanism in Scheme 3 for the **Ni-1***/SO_2/O_2 reaction.

Catalytic SO_2 Oxidation to SO_4^{2-}

Attempts to deploy the inexpensive NaSPh thiolate and nickel catalysis of the SO_2 to SO_4^{2-} conversion were carried out. The control experiment of SO_2/O_2 and NaSPh in the absence of metal complexes did not yield $BaSO_4$; however, the presence of the metal dithiolate complexes as well as simple salts such as $NiCl_2$ and $NiSO_4$ gave more than 100% yields (based on metal) of sulfate according to eq 3. Table 4 lists conditions and yields after 1 day of reaction. No further reaction was observed, and only **Ni-1*** and **Ni-2** were recovered (in ca. 80% yield). The others became inactive polymeric thiolates, sulfides, or oxides.

$$SO_2 + O_2 + 2SPh^- \xrightarrow{[Ni^{2+}]} SO_4^{2-} + PhSSPh \qquad (3)$$

The effectiveness of simple Ni^{2+} salts, $NiCl_2$, and $NiSO_4$, Table 4, suggests a requirement of SPh^- anion coordination to the metal, which then reacts with SO_2/O_2. The lower efficiency of the N_2S_2 and P_2S_2 tetradentate dithiolates probably reflects the lack of access of the SPh^- to Ni. The design of catalysts for this reaction would have the exacting demand of thiolate binding to metal without aggregation.

Conclusion

The organized, minimal step assembly of $SO_2/O_2/2e^-$ to form SO_4^{2-}, which has been established for two-electron, inner sphere reductants such as Ir^I in organometallic ligand environments, has been duplicated in thiolate complexes of nickel(II) and palladium(II). Unlike the metal-based organometallic systems, there is no oxidation state change of the metals in the group VIII thiolates, but rather the electron source is the thiolate ligands, resulting in S-oxidation and thiyl radical coupling to form disulfide. A similarity with metal-based analogues is the ability of the Pd and Ni thiolates to interact with or form adducts with both SO_2 and O_2, albeit at sulfur rather than metal. Structure/function relationships establish that it is the ability of these metal thiolates to react with O_2 and produce sulfur-oxygenated products (i.e., transfer S-electrons to oxygen) which provides a crucial connection to the SO_4^{2-} formation reaction. Nevertheless, the slow reactivity of stable metal-bound S-oxygenates with SO_2 eliminated the mechanistic possibility of isolable S-oxygenates as intermediates in the sulfate-producing reaction. Rather, it is proposed that a precursor O_2 adduct at sulfur, a sulfperoxide species, interacts with SO_2 with subsequent electron flow to yield SO_4^{2-} and disulfide. Initial studies employing metal thiolates as catalysts for the SO_2 oxygenation to SO_4^{2-} using exogenous thiolates as electron source find that the catalytic activity relies on the activation or binding of thiolate by the metal center.

Acknowledgment. Financial support from the National Science Foundation (CHE 91-09579 and 94-15901) for this work and for the X-ray diffractometer and crystallographic computing system (CHE-8513273) and contributions from the R. A. Welch Foundation are gratefully acknowledged. We thank Mr. Sandeep Bhatt and Ms. Tsung-Yen Tsai for help with the thermogravimetric analysis.

Supporting Information Available: Tables of crystallographic data collection parameters, atomic coordinates, and equivalent isotropic displacement parameters, complete listings of bond lengths and bond angles, anisotropic displacement parameters, H atom coordinates, and isotropic displacement parameters, and packing diagrams for complexes **Pd-1** and **Pd-1**·SO_2 (14 pages). This material is contained in many libraries on microfiche, immediately follows this article in the microfilm version of the journal, and can be ordered from the ACS; see any current masthead page for ordering information.

IC950664N

(40) Tuntulani, T.; Reibenspies, J. H.; Farmer, P. J.; Darensbourg, M. Y. *Inorg. Chem.* **1992**, *31*, 3497.
(41) Mills, D. K.; Hsiao, Y. M.; Farmer, P. J.; Atnip, E. V.; Reibenspies, J. H.; Darensbourg, M. Y. *J. Am. Chem. Soc.* **1991**, *113*, 1421.